Reprocessing the historical satellite passive microwave record at enhanced spatial resolutions using image reconstruction

M. A. Hardman[1], (molly.hardman@nsidc.org), M. J. Brodzik[1], D. G. Long[2], A. Paget[3], R. L. Armstrong[1]
[1]National Snow & Ice Data Center/CIRES, University of Colorado at Boulder, [2]Microwave Earth Remote Sensing Laboratory, BYU,
[3]Department of Marine Sciences, University of Connecticut

AGU Fall Meeting 14-18 December 2015
GC31D-1218

http://nsidc.org/pmesdr

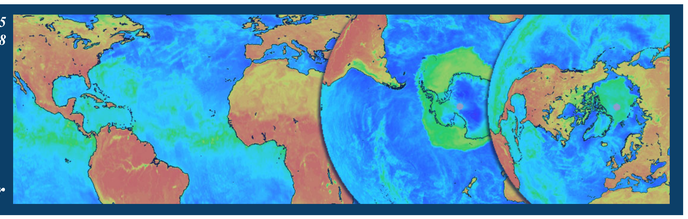

Objective

We are applying image reconstruction methods to produce a systematically reprocessed historical time series NASA MEaSUREs Earth System Data Record (ESDR), at higher spatial resolutions than have previously been available, for the 36-year satellite passive microwave record from SMMR, SSM/I-SSMIS and AMSR-E. We describe the general approach of two image reconstruction techniques: Backus-Gilbert (BG, Backus and Gilbert, 1967) and a radiometer version of the Scatterometer Image Reconstruction algorithm (SIR, Long and Daum, 1998; Early and Long, 2001). We include sample images at low and enhanced resolutions.

Image Reconstruction

Both BG and SIR transform radiometer data from swath to gridded format; both methods trade off between noise and spatial resolution. Our ESDR includes conventional low-noise, low-resolution gridded images (denoted GRD) and enhanced-resolution images with potentially higher noise.

For both GRD and enhanced resolution images, the effective gridded image resolution depends on the number of measurements and the precise details of their overlap, orientation, and spatial locations.

The goal of image reconstruction algorithms is to estimate brightness temperatures at fixed gridded locations, $T_B(x,y)$, from irregularly-located swath measurements, T_i. We define $R(x,y;\varphi_i)$ as the measurement response function (MRF) for a given channel and location. Then for a particular measurement T_i the sum of MRF weights is 1 and T_i can be written as:

$$T_i = \iint_{surface} R(x,y;\phi_i) T_B(x,y)\,dx\,dy$$

Each measurement T_i is treated as an MRF-weighted average of gridded T_Bs.

Ideally, the model requires knowledge of the sensor antenna pattern for the channel. In practice, this information is not available for every sensor. We approximate the MRF with a rotated, two-dimensional Gaussian function aligned with the elliptical footprint orientation (Long, 2015).

We have evaluated GRD, BG and SIR using a synthetic "truth" image, with features that simulate different target sizes, shapes and brightness gradients (Long and Brodzik, 2016). SIR is an iterative technique; it is tuned by number of iterations (N_i). BG is tuned by choice of the parameter gamma (γ), which ranges from 0 to $\pi/2$. Tuning parameters trade off between signal error and noise error. After analyzing noise performance for various choices of iteration number and pixel size (not shown here), we propose using: for BG, γ'=0.85; for SIR, N_i=20 and pixel sizes of 12.5, 6.25 or 3.125 km, depending on channel.

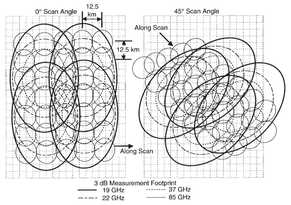

Geometry of radiometer measurement footprints for several along-track measurements for two different scan locations. Enhanced resolution images are produced on the underlying rectilinear grid (Long and Daum, 1998).

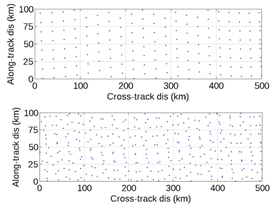

Example measurement locations within a small area of a SSM/I swath. Locations for a single orbit pass (top). Locations for two passes (bottom). Image reconstruction takes advantage of irregularly-spaced locations.

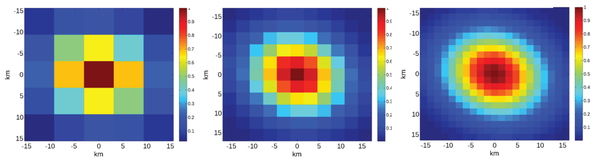

Illustration of a sampled MRF for different pixel sizes for the 85 GHz SSM/I channel, for 6.25 km pixels (left), 3.125 km pixels (center) and 1.5625 km pixels (right).

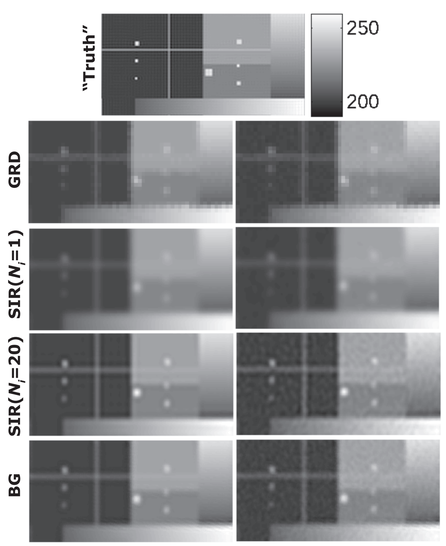

SSM/I 37 GHz simulation results. The 'true' brightness temperature image (top panel). Noise-free simulation results (left column). Noisy simulation results (right column). 25 km GRD (top row). AVE (SIR for iteration 1, second row). SIR (20 iterations, third row). BG with γ = 0.85 π/2 (bottom row).

Sensor name	Channels used	GRD pixel size (km)	Pixel size scale factor (N_a) and size (km)	SIR iterations	BG $g = \gamma/\pi$
SMMR	6.6H, 6.6V	25	(1) 12.50	20	0.85
	10.7H, 10.7V, 18H, 18V, 21H, 21V, 37H, 37V	25	(2) 6.250	20	0.85
SSM/I	19H, 19V, 22V, 37H, 37V,	25	(2) 6.250	20	0.85
	85H, 85V	25	(3) 3.125	20	0.85
SSMIS	19H, 19V, 22V, 37H, 37V	25	(3) 3.125	20	0.85
	91H, 91V	25	(3) 3.125	20	0.85
AMSR-E	6.9H, 6.9V	25	(2) 6.250	20	0.85
	10.7H, 10.7V, 18,7H, 18.7V, 23.8H, 23.8, 36.5H, 36.5V	25	(2) 6.250	20	0.85
	89H, 89V	25	(3) 3.125	20	0.85

Image reconstruction parameters used for candidate sensors.

Examples

During image reconstruction, each pixel brightness temperature is determined as a combination of all measurements within a certain spatio-temporal neighborhood, respectively weighted by the MRF of each measurement.

Sample images demonstrate low-noise, 25 km GRD vs. enhanced-resolution, 3.125 km SIR Northern Hemisphere *EASE-Grid 2.0* results for SSM/I 37 GHz, H-pol, morning passes from 1997 day 061.

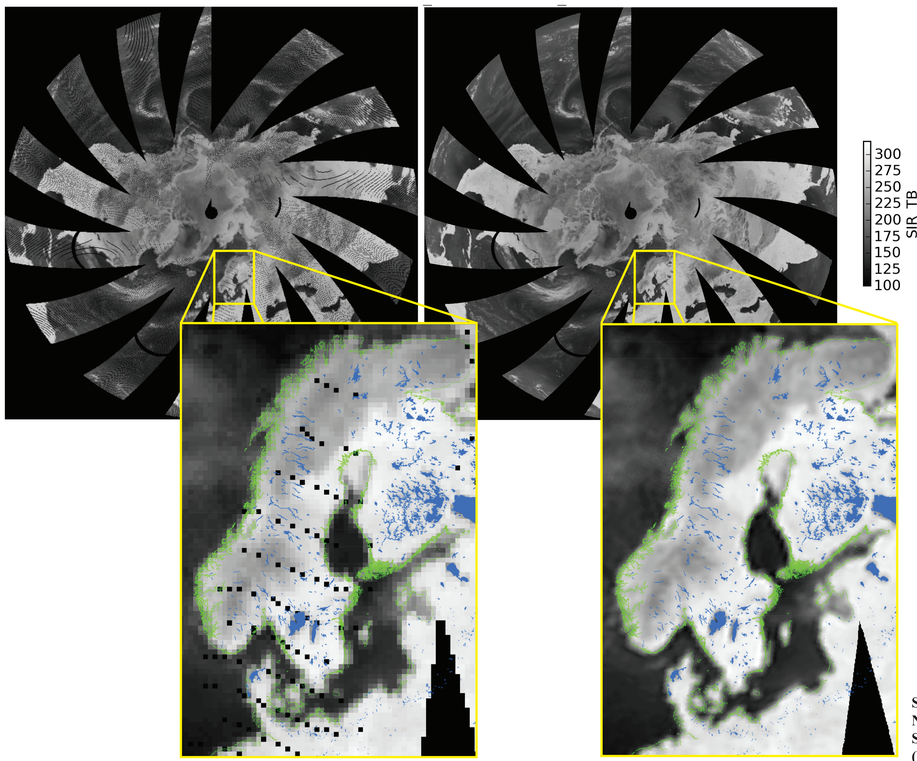

Sample GRD (left) and SIR (right) images for Northern Hemisphere, with zoomed detail in Scandinavia, overlaid with coastlines and lakes (Wessel and Smith, 2015).

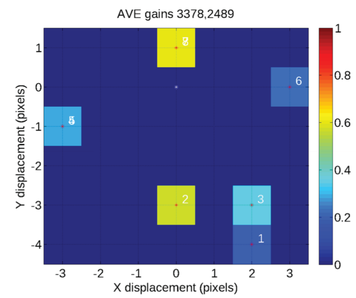

Relative displacements and SIR algorithm gains for each measurement that influences the pixel at location (0,0) of the study region.

Conclusions and Plans

While both BG and SIR enhance noise somewhat, we find that each can be tuned to produce higher-quality images (lower RMS image error) than conventional drop-in-the-bucket GRD images. SIR requires significantly less processing power than BGI.

We are producing a prototype ESDR including GRD, BG and SIR results for evaluation and feedback from our volunteer Early Adopter community. Our final ESDR will include 25 km GRD *EASE-Grid 2.0* images (Brodzik et al., 2012; 2014) and enhanced resolution grids (6.25 or 3.125 km) from either BG or SIR. Final choice of BG or SIR will depend on Early Adopter responses. If you are interested in being an Early Adopter, please contact us (*brodzik@nsidc.org*).

We anticipate that using our new brightness temperature ESDR may improve derived geophysical products in at least three ways:

1) we are using the latest intersensor calibration from Level 2 input data sets,
2) we are tuning image reconstruction parameters to enhance spatial resolution,
3) we will produce consistently gridded image products for the complete sensor record (SMMR, AMSR-E, 6 SSM/I and at least 2 SSMIS).

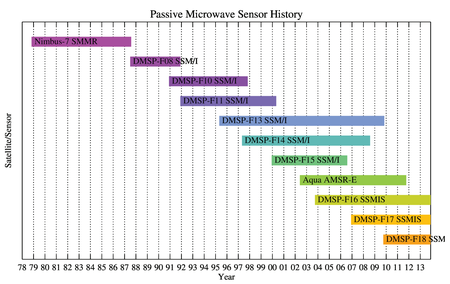

Availability of SMMR, AMSR-E, SSM/I and SSMIS sensors (dates are approximate); DMSP-F19 launched 3 Apr 2014 and F20 is not yet launched.

References and Acknowledgements

Backus, G. E. and J. F. Gilbert. 1967. Numerical applications of a formalism for geophysical inverse problems. Geophys. J. R. Astron. Soc., 13:247–276.
Brodzik, M. J., B. Billingsley, T. Haran, B. Raup, M. H. Savoie. 2012. EASE-Grid 2.0: Incremental but significant improvements for Earth-gridded data sets. ISPRS International Journal of Geo-Information, 1(1):32-45, doi:10.3390/ijgi1010032. http://www.mdpi.com/2220-9964/1/1/32/.
Brodzik, M. J., B. Billingsley, T. Haran, B. Raup, M. H. Savoie. 2014. Correction: Brodzik, M. J. et al. EASE-Grid 2.0: Incremental but significant improvements for Earth-gridded data sets. ISPRS International Journal of Geo-Information 2012, 1, 32-45. ISPRS International Journal of Geo-Information, 3(3):1154-1156, doi:10.3390/ijgi3031154. http://www.mdpi.com/2220-9964/3/3/1154/.
Early D. S. and D. G. Long. 2001. Image Reconstruction and Enhanced Resolution Imaging from Irregular Samples. IEEE TGARS, 39(2):291-302.
Long, D. G. 2015. An investigation of Antenna Patterns for the CETB. MEaSUREs Project White Paper, NSIDC. Boulder, CO. http://nsidc.org/pmesdr/files/2015/04/Long_20150302_CETB_Antenna_Patterns.v1.1.pdf.
Long, D. G. and M. J. Brodzik. 2016. Optimum image formation for spaceborne microwave radiometer products. IEEE TGARS, to Appear, doi:10.1109/TGARS.2015.2505677.
Long, D. G. and D. L. Daum. 1998. Spatial resolution enhancement of SSM/I data. IEEE TGARS, 36(2):407-417.
Wessel, P. and W. H. F. Smith. 2015. A Global, Self-Consistent, Hierarchical, High-Resolution Geography Database, V2.3.4. http://www.soest.hawaii.edu/pwessel/gshhg.

This work has been funded by NASA MEaSUREs 2012. We use the Janus supercomputer, which is supported by the National Science Foundation (award number CNS-0821794) and the University of Colorado Boulder. The Janus supercomputer is a joint effort of the University of Colorado Boulder, the University of Colorado Denver and the National Center for Atmospheric Research.